MECHANICAL BEHAVIOR INVESTIGATION OF LONGMAXI SHALE UNDER HIGH TEMPERATURE AND HIGH CONFINING PRESSURE

by

Hui-Jun LU[a,b], Dong-Feng HU[c], Ru ZHANG[a,d], Cun-Bao LI[d], Jun WANG[d], and Li REN[d*]

[a] State Key Laboratory of Hydraulics and Mountain River Engineering, Sichuan University, Chengdu, China
[b] College of Water Resource and Hydro Power, Sichuan University, Chengdu, China
[c] Sinopec Exploration Company, Chengdu City, Sichuan Province, China
[d] Key Laboratory of Deep Earth Science and Engineering (Sichuan University), Ministry of Education, Chengdu, China

Original scientific paper
https://doi.org/10.2298/TSCI180823219L

Triaxial compression tests are conducted on Longmaxi shale under high temperature and high confining pressure condition corresponding to a depth of 3000 m for two typical bedding plane orientations (0° and 90°). It is found that the crack initiation stresses and crack damage stresses of the Longmaxi shale specimens with different vein orientations are different, reflecting that the inclination of the bedding plane has a non-negligible influence on the microcrack initiation and propagation. In addition, the brittleness index of the Longmaxi shale with a bedding plane orientation of 90° is greater than that with an orientation of 0°, which confirmed that the brittleness index is related to the structural orientation under a high temperature and high confining pressure condition. Concerning the failure patterns, both the shear and tensile fracture modes has been observed.

Key words: *high temperature, high confining pressure, shale, brittleness, failure*

Introduction

Shale reservoirs in China are mainly concentrated at depths of 2500~4500 m [1]. In deep shale reservoirs, engineering practices showed that such an environment of high temperature and high stresses brings a great challenge in reservoir volume stimulating. The essential reason is that the high temperature and high confining pressure (HTHCP) condition controls the mechanical properties of shale rock. Therefore, an insight on the mechanical properties of shale rocks under a HTHCP condition is critical for stimulation treatments in deep shale reservoirs.

Due to the existing of veins, the shale is usually treated as a transversely isotropic material [2, 3]. To investigate the effect of veins on crack propagation in shale, several three-points-bending tests on shale specimens were conducted in [4]. The directional anisotropy in the compressive strength, tensile strength, elastic modulus and Poisson's ratio was reported in [5-8]. It should be mentioned that the tests were conducted without the consideration of confining pressure and temperature condition. Under different confining pressures, triaxial compression tests were carried out on shale in [9-11], showing that the compressive strength of shale increases with increasing confining pressure, and the resultant anisotropic characteristic of the

* Corresponding author, e-mail: renli-scu@hotmail.com

mechanical properties of shale is obvious. The mechanical properties of shale under different temperatures were investigated in [12]. Although the mechanical behaviors of shale under serials of temperature or confining pressure conditions have been investigated, the in-situ temperature and stress environment corresponding to a specific depth are not considered in the previous studies. Up to now, quite a few publications investigated the mechanical properties of shale under a coupled temperature and confining pressure condition. Therefore, the failure behaviors of shale in a deep environment are still unclear. Some experiments to research mechanical properties of shale under coupled temperature and confining pressure conditions were performed in [13, 14]. However, they used an experimental confining pressure ranging from 5 MPa to 25 MPa, which was considerably lower than the ground pressure of deep shale reservoirs.

Motivated by the previous results, the main aim of the paper is to present that the triaxial compression tests are conducted on Longmaxi shale under HTHCP conditions corresponding to a depth of 3000 m for two typical bedding plane orientations (0° and 90°). The influence of HTHCP on the mechanical properties and failure behavior of Longmaxi shale with different bedding plane orientations is discussed. Meanwhile, the brittleness index, elastic parameters, crack initiation stresses and crack damages stress of deeply buried shale is further obtained and analyzed to provide the reliable data for the design of the reservoir volume stimulating.

Experimental procedure

Rock samples

The Longmaxi shale blocks with obvious veins are collected for this experiment from Chongqing, Southwest China. To investigate the bedding effect, standard cylindrical samples with different bedding plane orientations (0° and 90°) are cored from a big block of Longmaxi shale.

Temperature, confining pressure and test procedure

Based on the well logging report of formation temperature and geo-pressure in the studied area, the experimental temperature and confining pressure are easily determined for a specific depth. Generally, the formation temperature increases linearly with depth:

$$T = t_0 + \frac{\partial t}{\partial H} H \tag{1}$$

where T is the formation temperature, t_0 – the surface temperature, $\partial t/\partial H$ – the temperature gradient, and H – the formation depth. The annual average surface temperature of the area is 18 °C. The temperature gradient is 2.43 °C/hm. Therefore, the temperature at a depth of 3000 m can be estimated as 90.93 °C by eq. (1). The minimum horizontal stress of the shale gas reservoir at a depth of 3000 m is 69.82 MPa. Consequently, confining pressure is set to 69.82 MPa.

The MTS 815 rock mechanics test system was used to carry out the HTHCP triaxial compression tests on the Longmaxi shale. To avoid the thermal stress concentration of the shale samples caused by excessive heating, the desired temperature is reached by heating at a constant rate of 12 °C/h. Then, after desired confining pressure is reached, tests are performed under strain controlled until the specimen is totally broken.

Results and analysis

Stress-strain curve characteristics

The stress-strain curves of the Longmaxi shale with different bedding plane orientations (0° and 90°) are shown in fig 1, which can be divided into four stages under HTHCP conditions.

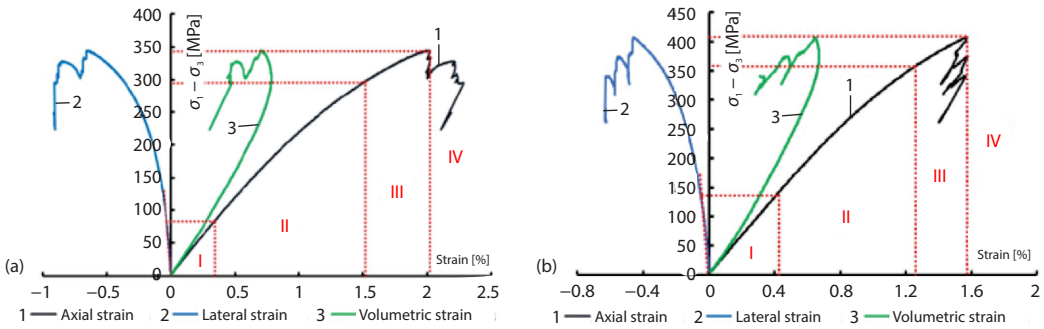

Figure 1. Stress-strain curves of Longmaxi shale for different bedding plane orientations; (a) $\theta = 0°$, (b) $\theta = 90°$

For the linear elastic deformation stage, Stage I, only a few primary microcracks are present or the primary microcracks are basically closed. Concerning the stable microcrack propagation stage, Stage II, the internal microcracks of the Longmaxi shale begin to propagate stably once the axial stress reaches the crack initiation stress. The previous linear elastic deformation stage is no longer maintained. Meanwhile, the slope of the stress-strain curve is slowly decreasing during this stage. With the propagation of the microcracks, a volume-expanding phenomenon will occur in the Longmaxi shale, reflected in the unstable microcrack propagation stage, Stage III. The sample is nearing the destruction stage. For Stage IV, when the microcracks develop into macroscopic cracks, the bearing capacity is reduced, and the axial stress rapidly reaches the peak strength and then decreases with a sudden drop (which indicated a brittle fracture behavior). In general, the deformation characteristics for the two bedding plane orientations (0° and 90°) are basically the same under HTHCP conditions. The stress-strain curves are typical type-II curves.

Strength characteristics

Shale mineral and particle distributions, especially the bedding structures formed by the orientation of clay minerals during the deposition process [15, 16]. Therefore, elastic parameters and strength of shale are significantly anisotropic. The nominal elastic modulus, E, and Poisson's ratio, v, are computed using straight parts (20-50% peak stress stage) of the stress-strain curves. The obtained strength, nominal elastic modulus and Poisson's ratio of Longmaxi shale with the orientation of 90° are greater than those with an orientation of 0° under HTHCP conditions. As shown in tab. 1. The anisotropy ratios of the elastic modulus and strength are 1.45 and 1.15, respectively.

Table 1. Strength, nominal elastic modulus, and Poisson's ratio

θ [°]	σ_f [MPa]	E [GPa]	v
0	414.01	21.97	0.18
90	476.32	31.79	0.19

The crack initiation stress, σ_{ci} and crack damage stress, σ_d, during loading are very important in investigating mechanical behaviors of rocks. As previously stated, the crack initiation stress represents the stress level that the occurence of the stable growth of micro-cracks, whereas the crack damage stress means that the micro-cracks starts to unstably propagate. That is saying the crack initiation and damage stresses could, to some extent, reflect the weakening process of a given rock. In this paper, these two stresses are determined based on the crack volumetric strain method [17, 18]. When deformation is in an elastic stage, the elastic volumetric strain is approximately equal to the total volumetric strain. When deformation is reflected in the stable microcrack propagation stage, the crack volume begins to increase, following the crack

initiation stress. With the propagation of microcracks and slippage of the internal cracks of the rock, a volume-expansion phenomenon occurs. The total volumetric strain-axial stress curve will have an inflection point, which corresponds to the crack damage stress.

The total volumetric strain of the shale can be assumed to be composed of the elastic volumetric strain and crack volumetric strain [18] *i. e.*:

$$\varepsilon_V = \varepsilon_{eV} + \varepsilon_{cV} = \varepsilon_1 + 2\varepsilon_3 \tag{2}$$

where ε_V is the total volumetric strain, ε_{eV} – the elastic volumetric strain, ε_{cV} – the crack volumetric strain, ε_1 – the axial strain, and ε_3 – the circumferential strain. The elastic volumetric strain [18]:

$$\varepsilon_{eV} = \frac{1-2v}{E}(\sigma_1 - \sigma_3) \tag{3}$$

where v is Poisson's ratio, E – the elastic modulus, σ_1 – the axial stress, and σ_3 – the confining stress. From eqs. (2) and (3) the crack volumetric strain can be written [18]:

$$\varepsilon_{cV} = \varepsilon_1 + 2\varepsilon_3 - \frac{1-2v}{E}(\sigma_1 - \sigma_3) \tag{4}$$

According to eq. (4), the crack volumetric strain-axial stress curve of Longmaxi shale can be obtained under HTHCP conditions, as shown in fig. 2. The obtained crack initiation stress and damage stress of the Longmaxi shale with different bedding plane orientations (0° and 90°) are summarized in tab. 2.

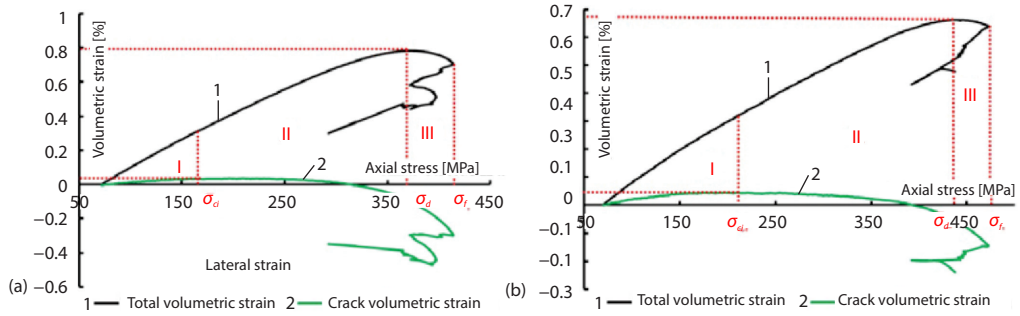

Figure 2. Stress-volumetric strain curves for different bedding plane orientations; (a) $\theta = 0°$, (b) $\theta = 90°$

Table 2. Physical and mechanical parameters of the Longmaxi shale

θ [°]	σ_{ci} [MPa]	σ_d [MPa]	σ_{ci}/σ_f [%]	σ_d/σ_f [%]
0	157.33	368.22	38.0	88.9
90	210.04	422.39	44.1	88.7

As indicated in tab. 2, the crack initiation stress and crack damage stress of the Longmaxi shale with an orientation of 90° are greater than those with an orientation of 0°. For shale rocks, the micro-cracks in the matrix will ultimately determine the crack initiation stress and weak planes will initiate and propagate separately. As known, the strength of weak plane is much lower than that of matrix. Therefore, the micro-cracks in weak planes will initiate and propagate at a relatively low stress level. Consequently, the sample with a 0° vein angle usually possesses lower strength, crack initiation stress and crack damage stress.

Brittleness index

The brittleness index is a crucial index for fracability evaluating of shale reservoir. Up to now, many methods were proposed to calculate the brittleness index. Referring to the methods

proposed by Rickman *et al*. [17] and Guo [19], the brittleness index of Barnett shale was calculated using its elastic modulus and Poisson's ratio. Meanwhile, it was reported that the elastic modulus and Poisson's ratio of Longmaxi shale in the Sichuan Basin range from 8-56 GPa and from 0.1- 0.36, respectively, [20]. The brittleness indexes for Longmaxi shale are modified [20]:

$$B_{RIT-\mathrm{E}} = \frac{E-8}{56-8}100 \tag{5}$$

$$B_{RIT-\nu} = \frac{\nu-0.36}{0.1-0.36}100 \tag{6}$$

$$B_{RIT-T} = \frac{B_{RIT-\mathrm{E}} + B_{RIT-\nu}}{2} \tag{7}$$

where $B_{RIT\text{-}E}$ is the normalized dynamic elastic modulus, $B_{RIT\text{-}v}$ – the normalized dynamic Poisson's ratio, and $B_{RIT\text{-}T}$ – the brittleness index.

Using eqs. (5)-(7), the brittleness index of the Longmaxi shale can then be calculated. For a bedding plane orientation of 0°, and 90°, the brittleness index is 49.16 and 57.5, respectively. This result indicates that the brittleness index of Longmaxi shale is related to the structural orientation under HTHCP conditions. Therefore, it is not enough to calculate the brittleness index only using some parameters for an arbitrarily chosen vein angle. For engineering practice, to better evaluate the fracability of shale reservoir, it is obvious that a lower brittleness index should be adopted. Meanwhile, the plastic properties of the Longmaxi shale are enhanced under HTHCP conditions, as shown in fig 1. As a result, it is not sufficient to use the elastic parameters to determine the brittleness index.

Failure behaviors

The failure modes of Longmaxi shale are closely related to the loading conditions, external environment and internal structural differences. The failure samples of the Longmaxi shale with different bedding plane orientations under the HTHCP conditions are shown in fig 3.

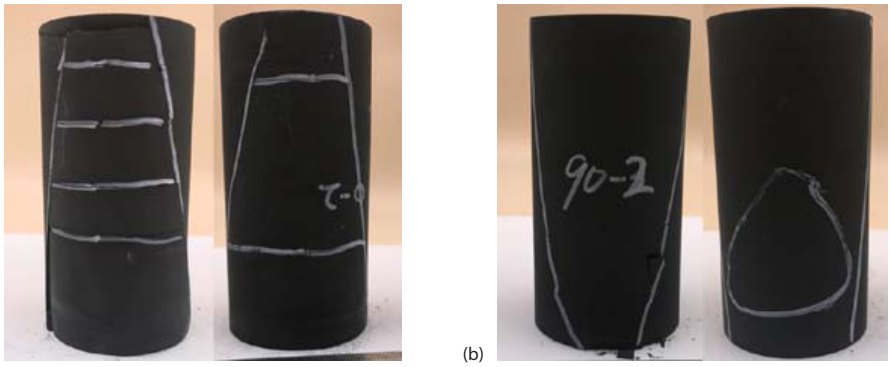

Figure 3. Broken samples of Longmaxi shale with different bedding plane orientations; (a) $\theta = 0°$, (b) $\theta = 90°$

For the orientation of 90°, the sample failures due to two main pairs of V-shaped macro-cracks in a shear failure mode, resulting in some cones. The top of the V-shaped shear plane is parallel to the bedding plane, which indicates a tensile splitting behavior. Flaking of curved fragments occurs on the flank of cone, which obliquely intersects the shear surface of cone. For the orientation of 0°, multiple tensile cracks form perpendicular to the bedding planes

and finally converge along the macro shear plane. As the axial stress increases, a potential plane of weakness is gradually activated and cohesion is gradually lost, resulting in the formation of cracks. Finally, this plane develops into a shear plane. For the tensile cracks in beddings, based on the stress-strain curve, the elastic deformation of the Longmaxi shale under compression is clearly dominant, resulting in considerable elastic energy accumulation before rock failure; this energy is released along a weak plane or microcracks on the post-peak stage. Consequently, tensile failure of a weak bedding plane is induced, creating a secondary crack.

Conclusion

The triaxial compression tests on Longmaxi shale were conducted for two typical bedding plane orientations under a high temperature and confining pressure corresponding to a depth of 3000 m. The results could be as the design and evaluation of stimulated reservoir volumes at a depth of 3000 m. Under a HTHCP condition, obvious non-linear deformation was observed for both orientation cases (0° and 90°). However, the ultimate failure of the investigated shale samples was brittle due the sudden drop of the stress-strain curves. The compressive strength, elastic modulus, Poisson's ratio, crack initiation stress and crack damage stress for a bedding plane orientation of 90° are greater than those for a bedding plane orientation of 0° under HTHCP condition. The calculated brittleness index of the Longmaxi shale with a bedding plane orientation of 90° is greater than that with an orientation of 0° and confirms that the brittleness index of the shale is related to the structural orientation under HTHCP conditions. Concerning the failure patterns, the shear and tensile fracture modes were observed for the two typical bedding plane orientations. Especially, the sudden releasing of the stored elastic strain energy inside a sample could lead up to a tensile interlaminar failure along the weak planes.

Acknowledgment

This work was supported by the National Natural Science Foundation of China (Grant No. 51622402 and No. 51704198), the department of Science and Technology of Sichuan Province (Grant No. 2017TD0007 and No. 2017HH0005) and national major science and technology project (Grant No. 2017ZX05036-003).

Nomenclature

$B_{RIT\text{-}E}$ – normalized dynamic elastic modulus,[–]
$B_{RIT\text{-}T}$ – brittleness index, [–]
$B_{RIT\text{-}v}$ – normalized dynamic Poisson's ratio, [–]
E – elastic modulus, [GPa]
H – formation depth, [m]
T – formation temperature, [°C]
t_0 – surface temperature, [°C]
$\partial t/\partial H$ – thermal gradient, [°Cm^{-1}]
v – Poisson's ratio, [–]

Greek symbols

ε_{cV} – crack volume strain, [–]
ε_{eV} – elastic volume strain, [–]
ε_V – total volume strain, [–]
ε_1 – axial strain, [–]
ε_3 – lateral strain, [–]
σ_{ci} – crack initiation stress, [MPa]
σ_d – damage stress, [MPa]
σ_1 – axial principle stress, [MPa]
σ_3 – confining pressure, [MPa]

References

[1] Jiang, F. J., *et al.*, the Main Progress and Problems of Shale Gas Study and the Potential Prediction of Shale Gas Exploration, *Earth Science Frontiers,19* (2012), Mar., pp. 198-211
[2] Amadei, B., Importance of Anisotropy when Estimating and Measuring in Situ Stresses in Rock, *International Journal of Rock Mechanics and Mining Sciences and GeoMechanics Abstracts, 33* (1996), 3, pp. 293-325
[3] Hakala, M., *et al.,* Estimating the Transversely Isotropic Elastic Intact Rock Properties For in Situ Stress Measurement Data Reduction: A Case Study of the Olkiluoto Mica Gneiss, Finland, *International Journal of Rock Mechanics and Mining Sciences, 44* (2007), 1, pp. 14-46

[4] Luo, Y., *et al.,* Linear Elastic Fracture Mechanics Characterization of an Anisotropic Shale, *Scientific Reports*, *8* (2018), 1, ID 8505
[5] Cho, J. W., *et al.,* Deformation and Strength Anisotropy of Asan Gneiss, Boryeong Shale, and Yeoncheon Schist, *International Journal of Rock Mechanics and Mining Sciences, 50* (2012), Feb., pp. 158-169
[6] Jia, C. G., *et al.,* Research on Mechanical Behaviors and Failure Modes of Layer Shale, *Rock Mechanics and Rock Engineering, 34* (2013), Oct., pp. 57-61
[7] Amann, F., *et al.,* Experimental Study of the Brittle Behavior of Clay Shale in Rapid Unconfined Compression, *Rock Mechanics and Rock Engineering, 44* (2011), 4, pp. 415-430
[8] Haghighat, E., *et al.*, Constitutive Modelling of Tournemire Shale, Report NO.RSP-0307, Canadian, Nuclear Safety Commission, Ottawa, Canada, 2015
[9] Niandou, H., *et al.,* Laboratory Investigation of the Mechanical Behavior of Tournemire Shale, *International Journal of Rock Mechanicals and Mining Sciences, 34* (1997), 1, pp. 3-16
[10] Ambrose, J., Failure of Shale under Triaxial Compressive Stress, Ph. D. thesis, Imperial College, London, UK, 2014
[11] Bonnelye, A., *et al.,* Strength Anisotropy of Shales Deformed under Uppermost Crustal Conditions, *Journal of Geophysical Research: Solid Earth, 122* (2017), 1, pp. 110-129
[12] Mohamadi, M., *et al.*, Strength and Post-Peak Response of Colorado Shale at High Temperature, *International Journal of Rock Mechanics and Mining Sciences, 84* (2016), Apr., pp. 34-46
[13] Masri. M., *et al.* Experimental Inverstigation of the Effect of Temperature on the Mechanical Behavior of Tournemire Shale, *International Journal of Rock Mechanics and Mining Sciences, 70* (2014), 9, Apr., pp. 185-191
[14] Meng, L. B., *et al.,* Experimental Study on Influence of Confining Pressure on Shale Mechanical Properties under High Temperature Condition, *Journal of China Coal Society, 37* (2012), 11, pp. 1829-1833
[15] O'Brien, N., *et al.*, *Argillaceous Rock Atlas*, Springer, New York, USA, 2012
[16] Johnston, J. E., *et al.*, Seismic Anisotropy of Shales, *Journal of Geophysical Research Solid Earth, 100* (1995), Apr., pp. 5991-6003
[17] Rickman, R., *et al.,* A Practical Use of Shale Petrophysics for Stimulation Design Optimization: All Shale Plays Are Not Clones of the Barnett Shale, *Proceedings*, SPE Annual Technical Conference and Exhibition, Denver, Col., USA, 2008, pp. 21-24
[18] Eberhardt, E., *et al.,* Quantifying Progressive Pre-Peak Brittle Fracture Damage in Rock during Uniaxial Compression, *International Journal of Rock Mechanics and Mining Sciences, 36* (1999), 3, pp. 361-380
[19] Guo, J. C., *et al*., A New Method for Shale Brittleness Evaluation, *Environmental Earth Sciences*, *70* (2015), 10, pp. 5855-5865
[20] Huang, J., *et al*., Shale Gas Accumulation Conditions and Favorable Zones of Silurian Longmaxi Formation in South Sichuan Basin, China, *Journal of China Coal Society*, *37* (2012), 5, pp. 782-787

Paper submitted: August 23, 2018
Paper revised: November 21, 2018
Paper accepted: February 27, 2019